Effects of mean-field and softening of equation of state on elliptic flow in Au+Au collisions at $\sqrt{s_{\rm NN}}=5$ GeV from the JAM model*

Jiamin Chen(陈佳敏)[1] Xiaofeng Luo(罗晓峰)[1,2;1)] Feng Liu(刘峰)[1] Yasushi Nara(奈良寧)[3,4]

[1] Institute of Particle Physics and Key Laboratory of Quark&Lepton Physics (MOE), Central China Normal University, Wuhan 430079, China
[2] Department of Physics and Astronomy, University of California, Los Angeles, California 90095, USA
[3] Akita International University, Yuwa, Akita-city 010-1292, Japan
[4] Frankfurt Institute for Advanced Studies, D-60438 Frankfurt am Main, Germany

Abstract: We perform a systematic study of elliptic flow (v_2) in Au+Au collisions at $\sqrt{s_{\rm NN}}=5$ GeV by using a microscopic transport model, JAM. The centrality, pseudorapidity, transverse momentum and beam energy dependence of v_2 for charged as well as identified hadrons are studied. We investigate the effects of both the hadronic mean-field and the softening of equation of state (EoS) on elliptic flow. The softening of the EoS is realized by imposing attractive orbits in two body scattering, which can reduce the pressure of the system. We found that the softening of the EoS leads to the enhancement of v_2, while the hadronic mean-field suppresses v_2 relative to the cascade mode. It indicates that elliptic flow at high baryon density regions is highly sensitive to the EoS and the enhancement of v_2 may probe the signature of a first-order phase transition in heavy-ion collisions at beam energies of a strong baryon stopping region.

Keywords: heavy-ion collisions, elliptic flow, equation of state, QCD phase transition

PACS: 25.75.-q, 25.75.Ld, 25.75.Nq **DOI:** 10.1088/1674-1137/42/2/024001

1 Introduction

Exploring the QCD phase transition is one of the main interests in current heavy-ion physics. Calculations from lattice QCD have shown that the transition from hadronic matter to quark-gluon plasma (QGP) is a crossover [1, 2] at vanishing baryon chemical potential ($\mu_B=0$), while a first-order phase transition is expected for finite baryon chemical potentials [3–5]. The first-order phase transition of QCD matter is related to the existence of a "softest point" in the equation of state (EoS), where the "softest point" in the EoS represents a local minimum of the ratio of the pressure to the energy density p/ε as a function of energy density ε [6, 7]. Collective flows have frequently been used to explore the properties of hot and dense matter [8, 9], since it can reflect the properties of the matter created in early stages of heavy-ion collisions and is expected to be sensitive to the EoS. Hydrodynamical calculations show a minimum in the excitation function of the directed flow around the softest point of the EoS, and this collapse of the directed flow is proposed as a possible signal of a first-order phase transition [10, 11].

Elliptic flow is also one of the most important observables which measures the momentum anisotropy of produced particles. In relativistic heavy-ion collisions at finite impact parameters, the particle momentum distribution measured with respect to the reaction plane is not isotropic and it is usually expanded in a Fourier series [12, 13]:

$$\frac{{\rm d}N}{{\rm d}(\phi-\psi)}=\frac{N}{2\pi}\left[1+2\sum_{n=1}^{\infty}v_n\cos[n(\phi-\psi)]\right], \tag{1}$$

where ϕ is the emission azimuthal angle of the particles and ψ is the reaction plane angle. The flow coefficients $v_n=\langle\cos n(\phi-\psi)\rangle$ are a quantitative characterization of the event anisotropy, where the symbol $\langle\ \rangle$ indicates an average over all particles and all events. The elliptic flow parameter is defined as the second Fourier coefficient v_2 of the particle momentum distributions and it can be expressed as

$$v_2=\langle\cos2(\phi-\psi)\rangle=\left\langle\frac{p_x^2-p_y^2}{p_x^2+p_y^2}\right\rangle, \tag{2}$$

where p_x and p_y are the x (impact parameter direction

Received 20 October 2017, Revised 27 November 2017, Published online 12 January 2018
* Supported by the MoST of China 973-Project (2015CB856901), NSFC (11575069, 11221504). Y. N. is supported by the Grants-in-Aid for Scientific Research from JSPS (15K05079, 15K05098)

1) E-mail: xfluo@mail.ccnu.edu.cn

on the reaction plane) and y (direction perpendicular to the reaction plane) components of the particle momenta, respectively. Elliptic flow is expected to arise out of the pressure gradient and subsequent interactions among the constituents in non-zero impact parameter collisions. Thus it provides plenty of information about the early-time thermalization and is a good tool to study the system formed in the early stages of high-energy nuclear collisions [14–17]. The elliptic flow is one of the most extensively studied observables in relativistic nucleus-nucleus collisions (for a review see Ref. [13]). The elliptic flow as a function of transverse momentum ($p_{\rm T}$), pseudorapidity (η), and centrality has been widely measured at different experiments in the last couple of decades [18–27]. Transport theoretical models are used to analyze the experimental data [28–34].

Although the characteristics of v_2 at high incident energies have been extensively investigated where one expects the creation of almost baryon free QGP, it is also of great interest to perform a corresponding research for high baryon density regions, and new experiments are planned such as BES II at RHIC [35], FAIR [36], J-PARC [37], and NICA [38]. In this work, we use a microscopic transport model, JAM [39–41], to systematically study the centrality, transverse momentum and pseudo-rapidity dependence of v_2 in Au+Au collisions at $\sqrt{s_{\rm NN}}$=5 GeV, which is the top center-of-mass energy of the Compressed Baryonic Matter (CBM) at SIS100 [42] heavy-ion collision experiment at FAIR. In the following, we shall investigate the effects of the mean field potential and the softening of EoS on the elliptic flow by employing the JAM transport model.

This paper is organized as follows. We provide a brief description of the JAM model on which our studies are based in Section 2. In Section 3, we show the transverse mass spectra of negative pions, nucleons and charged particles in $\sqrt{s_{\rm NN}}=5$ GeV Au+Au collisions. We also present our results on the centrality, transverse momentum, pseudorapidity, and beam energy dependence of elliptic flow for charged hadrons as well as protons, pions, kaons and their corresponding anti-particles. Finally, a summary of our work is given in Section 4.

2 The JAM model

Several microscopic transport models, such as RQMD [43], UrQMD [44, 45], AMPT [46], PHSD [47], and JAM [39], have frequently been used to explore (ultra-) relativistic heavy-ion collisions. JAM (Jet AA Microscopic Transport Model) has been developed based on resonance and string degrees of freedom [39], similar to the RQMD and UrQMD models, in order to simulate (ultra-)relativistic nuclear collisions from the initial stages of the reaction to final state interactions in the hadronic gas stage. In JAM, particles are produced via the resonance or string formations followed by their decays. Hadrons and their excited states are explicitly propagated in space-time by the cascade method [48].

We study the effect of hadronic mean-field potentials on elliptic flow by employing the JAM mean-field mode, in which hadronic mean-field potentials are implemented based on the framework of the simplified version of Relativistic Quantum Molecular dynamics (RQMD/S) [28]. The Skyrme type density dependent and Lorentzian-type momentum dependent mean-field potentials [49] for baryons are adopted in the RQMD/S approach, and the single-particle potential U has the form

$$U(\boldsymbol{r},\boldsymbol{p}) = \alpha\left(\frac{\rho(\boldsymbol{r})}{\rho_0}\right)+\beta\left(\frac{\rho(\boldsymbol{r})}{\rho_0}\right)^{\gamma} + \sum_{k=1,2}\frac{C_k}{\rho_0}\int \mathrm{d}\boldsymbol{p}'\frac{f(\boldsymbol{r},\boldsymbol{p}')}{1+[(\boldsymbol{p}-\boldsymbol{p}')/\mu_k]^2}, \quad (3)$$

where $f(\boldsymbol{r},\boldsymbol{p})$ is the phase space distribution function and $\rho(\boldsymbol{r})$ is the baryon density. The parameters α, β, γ, ρ_0, C_1, C_2, μ_1, μ_2 are taken from Ref. [40].

We also study the effect of the softening of EoS on elliptic flow by the method of choosing an attractive orbit in two-body scattering [41]. It is well known from the virial theorem [50] that attractive orbits in each two-body hadron-hadron scattering reduce the pressure of the system. We impose attractive orbits for all two-body scatterings, thus there is no free parameter in terms of the implementation of attractive orbit mode in JAM.

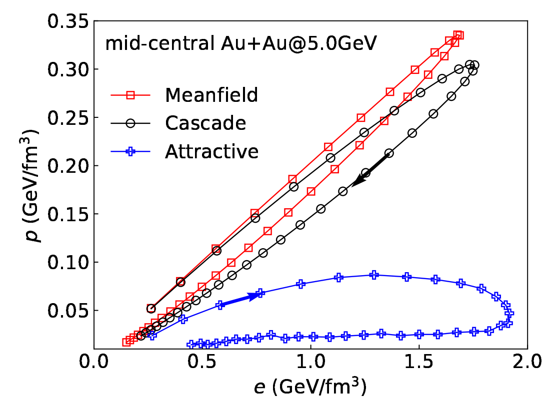

Fig. 1. (color online) Time evolution of pressure and energy density in mid-central Au+Au collisions at $\sqrt{s_{\rm NN}}=5$ GeV from JAM cascade (circles), attractive orbit (crosses), and mean-field mode (squares). Pressure and energy density are averaged over collision points in a cylindrical volume of transverse radius 3 fm and a longitudinal distance of 2 fm centered at the origin.

Figure 1 displays the time evolution of the local pressure and energy density extracted from the energy-momentum tensor for mid-central Au+Au collisions at

$\sqrt{s_{\rm NN}}=5$ GeV to see the difference of EoS in the three different modes in JAM. We observe that mean-field mode in JAM shows a harder EoS, while attractive orbit mode significantly lowers the pressure of the matter. We showed in Ref. [41] that attractive orbit simulation yields an amount of softening of the EoS compatible with the EOS-Q [51] first-order phase transition. It is also seen that highest maximum energy density is achieved in the attractive orbit mode in JAM due to soft compression of the matter, while mean-field mode yields the lowest energy density due to repulsive potential effects.

3 Results

In Fig. 2, rapidity distributions of protons and negative pions in mid-central collisions ($4.6<b<9.4$ fm) are shown. Those spectra are calculated by using three different modes in JAM, including the standard cascade, mean-field, and attractive orbit. There is no significant difference among the three modes except for a suppression of pion yield (5%) by the mean-field, which is well-known. As expected from the time evolutions of the EoS, attractive orbit mode in JAM slightly enhances the yields of both protons (8%) and pions (2%) at mid-rapidity, while at $y\geq\pm1$, the yields are less than the cascade mode, and integrated yield over rapidity remains the same.

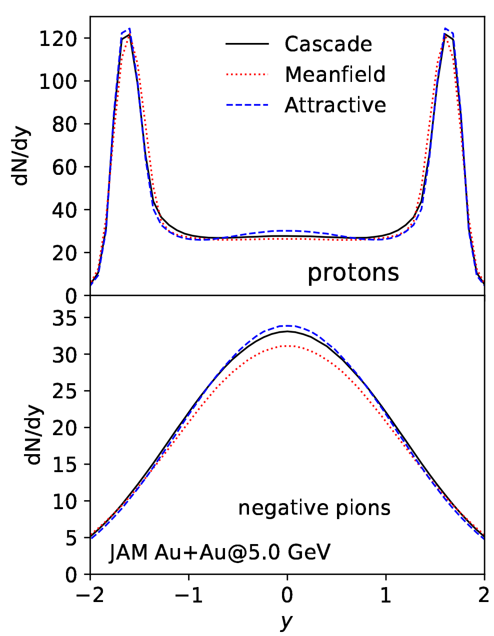

Fig. 2. (color online) Rapidity distributions of protons (top) and negative pion (bottom) in mid-central $\sqrt{s_{\rm NN}}=5$ GeV Au+Au collisions from JAM with three different modes.

In Fig. 3, we show the transverse mass spectra, $\frac{1}{2\pi m_{\rm T}}\frac{{\rm d}N}{{\rm d}m_{\rm T}{\rm d}y}$ at mid-rapidity $|y|<0.12$, for negative pions, nucleons and charged particles. By comparing with the standard JAM cascade, we find that both the mean-field and the attractive orbit modes enhance the transverse radial flow. Such enhancement of slope comes from different dynamical origins. The enhancement in the mean-field mode is due to the repulsive potential interactions, while in the case of attractive orbit mode, it is due to the creation of more compressed matter and soft expansion, which results in the longer lifetime of the system. Namely, with matter compressed and softer expansion, there are more interactions which create stronger radial flow. Note that the radial flow can be generated all the way from the early to late stages of collisions, unlike

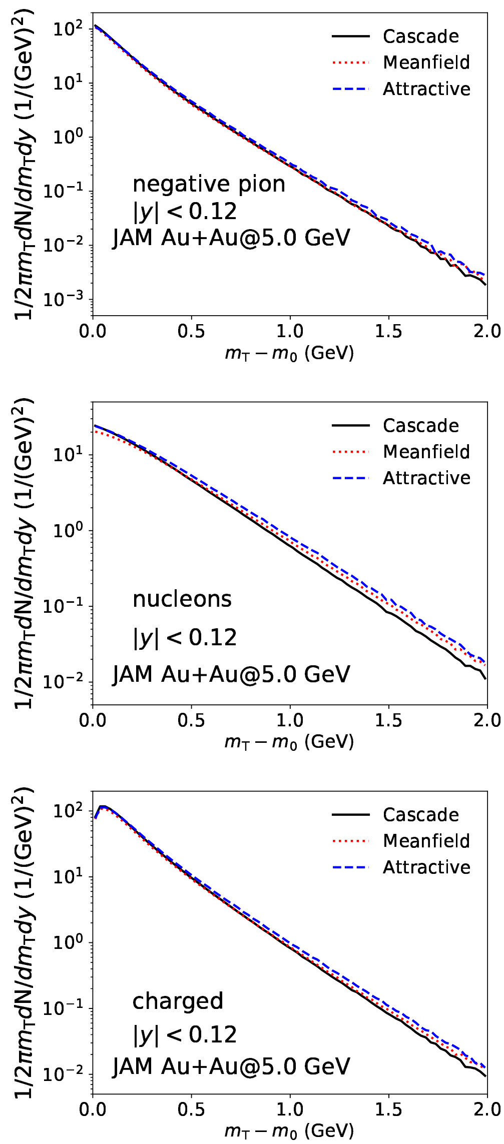

Fig. 3. (color online) Transverse mass spectra of negative pions (top), nucleons (middle) and charged particles (bottom) in mid-central $\sqrt{s_{\rm NN}}=$ 5 GeV Au+Au collisions from JAM with three different modes.

anisotropic flows, which are more sensitive to the early pressure. In addition, radial flow is proportional to the pdV work in the hydrodynamic approximation, thus is essentially proportional to the system size. On the other hand, early and late pressures contribute with opposite signs to the elliptic flow [14], as we will address below. We note that the enhancement of proton collective radial transverse flow by a first-order phase transition is also seen in the hydrodynamical simulations [52, 53] as consistent with our attractive orbit simulation in JAM.

Various methods are proposed to extract the Fourier coefficients of the particle momentum distributions, since the reaction plane is not known in heavy ion experiments. Before studying the systematics of elliptic flow, we compared two methods: the event plane [12] and the two-particle cumulant method [22, 54]. These methods were already applied to the JAM simulations [55] and it was found that they agree with each other. Here we also check these methods for attractive orbit mode in JAM. As seen in Fig. 4, both event plane elliptic flow $v_2\{\text{EP}\}$ and the cumulant elliptic flow $v_2\{2\}$ are in good agreement with the reaction plane elliptic flow v_2. This is consistent with the observation by the STAR collaboration at the BES energy region [25], in which elliptic flow from the four-particle cumulants method agrees with the values extracted from both two-particle cumulants and event plane methods for mid-central collisions at $\sqrt{s_{\text{NN}}}\leq 11.5$ GeV. Since we do not see any significant differences among different methods in our beam energy range, we consider the reaction plane elliptic flow below.

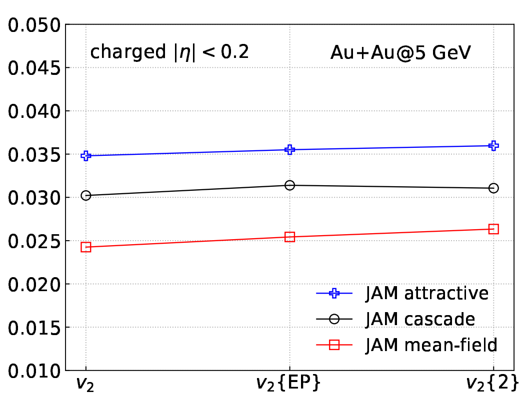

Fig. 4. (color online) Elliptic flow of charged hadrons from reaction plane v_2, event plane $v_2\{\text{EP}\}$, and cumulant method $v_2\{2\}$ at mid-rapidity ($|\eta|<0.2$) in mid-central ($4.6<b<9.4$fm) $\sqrt{s_{\text{NN}}}=5$ GeV Au+Au collisions from JAM with three different modes.

We now present the JAM results for the centrality, transverse momentum and pseudorapidity dependence of v_2 in Au+Au collisions at $\sqrt{s_{\text{NN}}}=5$ GeV. All results are computed directly from Eq. (2), taking the true reaction plane from the JAM model. The collision centrality is defined by the charged particle multiplicity within $|\eta|<1$.

Figure 5 shows the centrality dependence of charged hadron v_2 at mid-rapidity ($|\eta|<0.2$) in Au+Au collisions at $\sqrt{s_{\text{NN}}}=5$ GeV. As we can see, the magnitude of the elliptic flow v_2 in semi-central collisions (20%–30%) is the largest for all three modes, these being the cascade, mean-field and attractive orbit mode, respectively. The general trend of v_2 versus centrality for the mean-field and attractive orbit mode is similar to the cascade mode predictions. We observe that the mean-field reduces the values of charged hadron v_2 compared to the cascade mode in a way consistent with previous studies by transport models [8, 28], while the attractive orbits enhance the elliptic flow of charged hadrons. In the case of the mean-field mode, higher pressures are generated in the system due to the repulsive interactions which accelerate the expansion of the participant matter. As a result, spectator matter squeezes participant matter out-of-plane more than the cascade mode, which leads to the suppression of v_2 [8, 14]. We note that a different mechanism for the generation of negative v_2 has recently been proposed at lower beam energies around $E_{\text{kin}}\approx 1$ AGeV within the QMD approach [56].

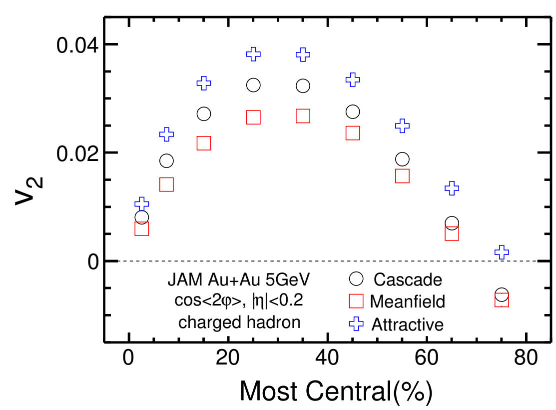

Fig. 5. (color online) The η ($|\eta|<0.2$) integrated v_2 of charged hadrons as a function of collision centrality in Au+Au collisions at $\sqrt{s_{\text{NN}}}=5$ GeV from the standard JAM cascade (circles), JAM with mean-field (squares), and JAM with attractive orbit (crosses).

However, the pressure is significantly reduced in the case of attractive orbit mode. Consequently, participant matter may expand much more slowly, which reduces the interactions with the spectator matter that results in the strong in-plane emission. This might be the reason we see the enhancement of v_2 in attractive orbit mode.

To gain more information about the effects of mean field and the softening of EoS on the elliptic flow, we study the elliptic flow of identified hadrons (p, π^+, K^+)

and their anti-particles in Au+Au collisions at $\sqrt{s_{\rm NN}}$=5 GeV. Since the yield of anti-protons produced at this beam energy in JAM is very small, the measurement of v_2 for antiproton has large statistical errors and we do not show the anti-proton v_2 in our results.

In Fig. 6, we show the centrality dependence of v_2 for particles (p, π^+, K^+, π^-, K^-) in Au+Au collisions at $\sqrt{s_{\rm NN}}$=5 GeV from the JAM model in the three different modes. We observe that v_2 calculated from the attractive orbit mode shows larger values for pions and kaons compared to the cascade mode, but proton v_2 is similar to the cascade mode. However, we find that the magnitude of v_2 from the mean-field mode is smaller than the results from the cascade mode for all particles in the mid-central region. Thus, the enhancement of charged hadron v_2 in the attractive orbit mode observed in Fig. 5 comes mainly from the changes of pion and kaon flows. We note that the JAM mean-field result for v_2 seems to be in good agreement with the experimental data from the top AGS energy $\sqrt{s_{\rm NN}}$=4.7 GeV [18].

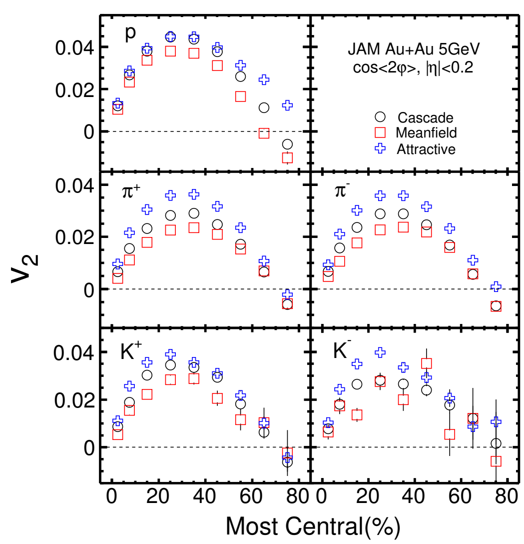

Fig. 6. (color online) The η ($|\eta|<0.2$) integrated v_2 as a function of collision centrality in Au+Au collisions at $\sqrt{s_{\rm NN}}$=5 GeV from JAM cascade model (circles), JAM cascade with mean-field (squares), and JAM cascade with attractive orbit (crosses). The left and right panels show the results for identified particles (p, π^+, K^+) and corresponding antiparticles (π^-, K^-), respectively.

Experimentally, the measured antiparticle v_2 is lower than the corresponding particle v_2 and the difference in v_2 between particles and their antiparticles should increase with decreasing beam energy [26]. However, JAM predicts that the values of v_2 for particles are similar to the results for their antiparticles. The similarity of the values of v_2 between particles and their anti-particles in JAM is due to the scalar type baryonic mean-field potentials implemented for all baryons, and no mean-field for pions and kaons. The Skyrme type density dependent potentials have been tested for a long time using the QMD and BUU microscopic transport models, and it is a reasonable approximation at the beam energies under consideration from the point of view of the tiny number of anti-baryons produced in the collision. In Ref. [31, 32], it is found that the different mean-field potentials among particles and their anti-particles in the hadronic as well as partonic phases improve the description of the data on the difference of v_2 between particles and their anti-particles observed in the STAR Beam Energy Scan (BES) program.

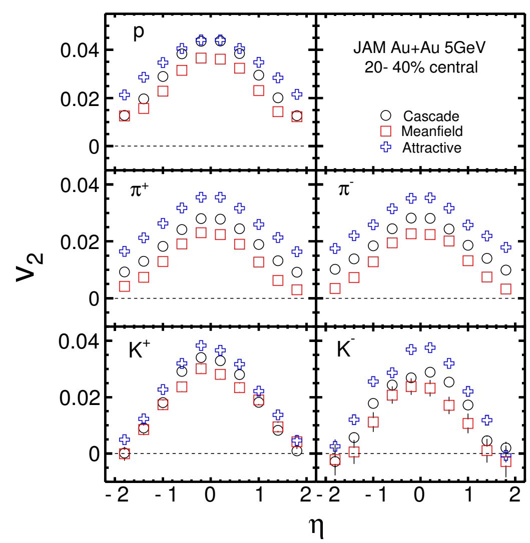

Fig. 7. (color online) v_2 as a function of η in 20%–40% mid-central Au+Au collisions at $\sqrt{s_{\rm NN}}=5$ GeV from JAM cascade model (circles), JAM cascade with mean-field (squares), and JAM cascade with attractive orbit (crosses). The left and right panels show the results for identified particles (p, π^+, K^+) and corresponding antiparticles (π^-, K^-), respectively.

We have also studied the pseudo-rapidity and transverse momentum dependence of v_2 in mid-central (20%–40%) Au+Au collisions. In Fig 7, the η dependence of v_2 for the particles (p, π^+, K^+) and corresponding antiparticles (π^-, K^-) are presented. The results of the JAM model for particles and antiparticles show a similar decreasing trend of v_2 with increasing $|\eta|$. We observe that the values of v_2 for pions and kaons from the attractive orbit mode are larger than those from the cascade mode, while v_2 for protons is similar to the cascade mode prediction at mid-pseudorapidity. At the same time, from our results it is clear that v_2 from mean-field mode is always smaller than the results from the cascade and attractive orbit modes for all the particles.

In Fig. 8, we show v_2 for identified particles as a function of the transverse momentum $p_{\rm T}$ for $|\eta|<0.2$ in 20%–40% mid-central Au+Au collisions at $\sqrt{s_{\rm NN}}=5$ GeV. The results from three different modes show a similar transverse momentum dependence in $v_2(p_{\rm T})$. It is also observed that the proton $v_2(p_{\rm T})$ from JAM standard cascade and JAM with attractive orbit modes are similar for the low $p_{\rm T}$ range. The results of $v_2(p_{\rm T})$ from the cascade and attractive orbit mode are larger than the result from JAM with the mean-field mode for pions. Although the statistical error on the kaon and antikaon is relatively large, the general increasing trend of $v_2(p_{\rm T})$ with increasing $p_{\rm T}$ is still obvious. The difference in $v_2(p_{\rm T})$ between the particles and corresponding antiparticles from JAM is small, as expected from the integrated v_2 results.

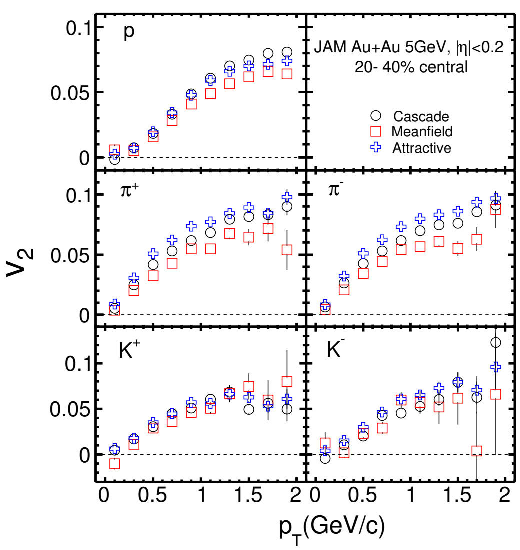

Fig. 8. (color online) v_2 as a function of the transverse momentum $p_{\rm T}$ for $|\eta|<0.2$ in 20-40% mid-central Au+Au collisions at $\sqrt{s_{\rm NN}}=5$ GeV from JAM cascade model (circles), JAM cascade with mean-field (squares), and JAM cascade with attractive orbit (crosses). The left and right panels show the results for identified particles (p, π^+, K^+) and corresponding antiparticles (π^-, K^-), respectively.

Finally, in Figure 9, we compute the beam energy dependence of the elliptic flow v_2 for charged hadrons at mid-rapidity. It is seen that v_2 from JAM attractive mode is always greater for all beam energies up to $\sqrt{s_{\rm NN}}=7.0$ GeV, and the effect of mean-field mode is to suppress v_2. We note that v_2 for charged hadrons above $\sqrt{s_{\rm NN}}=7.7$ GeV from the JAM attractive mode does not show any enhancement relative to the JAM standard cascade results [41], and the effects of hadronic mean-field on v_2 is very small at SPS energies [28]. Thus an enhancement of v_2 is predicted only at the beam energy lower than 7 GeV in JAM, which is due to the suppression of the squeeze-out effect by the softening of the EoS. It is known that microscopic hadronic transport model predictions including hadronic mean-field are consistent with the data up to the top AGS energy 4.7 GeV [8, 28, 57], thus the scenario of the phase transition seems to be ruled out at beam energies less than 5.0 GeV. However, there is no data between 5.0 and 7.7 GeV, and it is still interesting to measure the elliptic flow in this beam energy region experimentally, in order to investigate possible phase transition signals of strongly interacting matter created in heavy ion collisions.

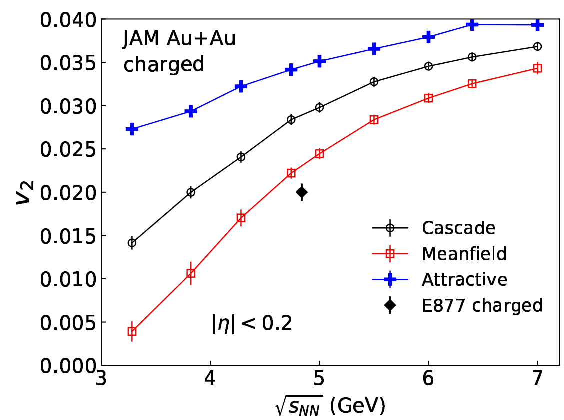

Fig. 9. (color online) Beam energy dependence of elliptic flow v_2 for charged hadrons for $|\eta|<0.2$ from JAM in mid-central Au+Au collisions ($4.6<b<9.4$ fm). Data is taken from Ref. [58].

4 Summary

We have studied the effects of the hadronic mean-field and the softening of the EoS on the elliptic flow in Au+Au collisions at $\sqrt{s_{\rm NN}}=5$ GeV within the JAM model. The calculations of v_2 were performed within three different modes, the cascade, mean-field, and attractive orbit modes. We observed that both mean-field and attractive orbit modes enhance the spectrum slope of nucleons and charged particles. However, we found that the value of v_2 from the attractive orbit mode is larger than the one from the cascade mode, while the mean-field mode yields lower v_2 than the results from the cascade mode. We have also presented the centrality, $p_{\rm T}$ and η dependence of v_2 for identified particles (p, π^+, K^+) and corresponding antiparticles (π^-, K^-), respectively. The magnitudes of v_2 from the JAM model for identified particles are similar to those for their antiparticles.

Our results indicate a high sensitivity of the elliptic flow to the pressure of the system. The hadronic mean-field generates more pressure which leads to a stronger squeeze-out effect. Furthermore, enhancement of the elliptic flow is predicted for the attractive orbit mode, which leads to softening of the EoS within the non-equilibrium microscopic simulations, the first time this effect has been predicted. The enhancement of v_2 is caused by a suppression of squeeze-out effects due to the lower pressure of the system. Our results suggest that enhancement of the elliptic flow in Au+Au collisions in the highest baryon density region may be used as a signal for a first-order phase transition. For further investigations in this direction, a study of the EoS dependence of the elliptic flow by the transport approach with the EoS modified collision term [59] may provide useful information.

References

1 Y. Aoki, G. Endrodi, Z. Fodor, S. D. Katz, and K. K. Szabo, Nature, **443**: 675 (2006)
2 C. Bernard, T.Burch, C. DeTar et al, Phys. Rev. D, **71**: 034504 (2005)
3 A. Masayuki, Y. Koichi, Nucl. Phys. A, **504**: 668 (1989)
4 P. Costa, M. C. Ruivo, and C. A. de Sousa, Phys. Rev. D, **77**: 096001 (2008)
5 S. Ejiri, Phys. Rev. D, **78**: 074507 (2008)
6 C. M. Hung and E.V. Shuryak, Phys. Rev. Lett., **75**: 4003 (1995)
7 D. H. Rischke and M. Gyulassy, Nucl. Phys. A, **608**: 479 (1996)
8 P. Danielewicz, R. Lacey, and W. G. Lynch1, Science, **298**: 1592 (2002)
9 H. Stoecker, Nucl. Phys. A, **750**: 121 (2005)
10 D. H. Rischke, Y. Puersuen, J. A. Maruhn, H. Stoecker, and W. Greiner, Heavy Ion Phys., **1**: 309 (1995)
11 J. Brachmann, S. Soff, A. Dumitru, H. Stoecker, J. A. Maruhn, W. Greiner, L. V. Bravina, and D. H. Rischke, Phys. Rev. C, **61**: 024909 (2000)
12 A. M. Poskanzer and S. A. Voloshin, Phys. Rev. C, **58**: 1671 (1998)
13 S. A. Voloshin, A. M. Poskanzer, and R. Snellings, In Relativistic Heavy Ion Physics, pages 293-333, Springer, 2010. [arXiv:0809.2949]
14 H. Sorge, Phys. Rev. Lett., **78**: 2309 (1997)
15 H. Sorge, Phys. Rev. Lett,. **82**: 2048 (1999)
16 D. Teaney and J. Lauret, and E. V. Shuryak, Phys. Rev. Lett., **86**: 4783 (2001)
17 U. Heinz, Nucl. Phys. A, **830**: 287 (2009)
18 C. Pinkenburg et al (E895 Collaboration), Phys. Rev. Lett., **83**: 1295 (1999)
19 C. Alt et al (NA49 Collaboration), Phys. Rev. C, **68**: 034903 (2003)
20 S. Afanasiev et al (PHENIX Collaboration), Phys. Rev. C, **80**: 024909 (2009)
21 A. Adare et al (PHENIX Collaboration), Phys. Rev. Lett., **105**: 062301 (2010)
22 C. Adler et al (STAR Collaboration), Phys. Rev. C, **66**: 034904 (2002)
23 B. I. Abelev et al (STAR Collaboration), Phys. Rev. C, **77**: 054901 (2008)
24 B. I. Abelev et al (STAR Collaboration), Phys. Rev. C, **81**: 024911 (2010)
25 L. Adamczyk et al (STAR Collaboration), Phys. Rev. C, **86**: 054908 (2012)
26 L. Adamczyk et al (STAR Collaboration), Phys. Rev. Lett., **110**: 142301 (2013)
27 L. Adamczyk et al (STAR Collaboration), Phys. Rev. C, **88**: 014902 (2013)
28 M. Isse, A. Ohnishi, N. Otuka, P. K. Sahu, and Y. Nara, Phys. Rev. C, **72**: 064908 (2005)
29 Md. Nasim, L. Kumar, P. K. Netrakanti, and B. Mohanty, Phys. Rev. C, **82**: 054908 (2010)
30 Md. Nasim, R. Esha, and H. Z. Huang, Phys. Rev. C, **93**: 044920 (2016)
31 J. Xu, C. M. Ko, F. Li and T. Song, and H. Liu, Nucl. Phys. Rev., **32**: 146 (2015)
32 J. Xu and C. M. Ko, Phys. Rev. C, **94**(5): 054909 (2016)
33 J. Auvinen and H. Petersen, Phys. Rev. C, **88**(6): 064908 (2013)
34 Y. B. Ivanov and A. A. Soldatov, Phys. Rev. C, **91**(2): 024914 (2015)
35 G. Odyniec, EPJ Web Conf., **95**: 03027 (2015)
36 C. Hhne (CBM Collaboration), J. Phys. Conf. Ser., **420**: 012016 (2013)
37 H. Sako et al, Nucl. Phys. A, **931**: 1158 (2014); H. Sako et al (J-PARC Heavy-Ion Collaboration), Nucl. Phys. A, **956**: 850 (2016)
38 V. Kekelidze, A. Kovalenko, R. Lednicky, V. Matveev, I. Meshkov, A. Sorin, and G. Trubnikov, Nucl. Phys. A, **956**: 846 (2016)
39 Y. Nara, N. Otuka, A. Ohnishi, K. Niita, and S. Chiba, Phys. Rev. C, **61**: 024901 (1999)
40 Y. Nara and A. Ohnishi, Nucl. Phys. A, **956**: 284 (2016)
41 Y. Nara, H. Niemi, A. Ohnishi, and H. Stoecker, Phys. Rev. C, **94**: 034906 (2016)
42 T. Ablyazimov, et al (CBM Collaboration), arXiv:1607.01487 [nucl-ex]
43 H. Sorge, Phys. Rev. C, **52**: 3291 (1995); Phys. Lett. B, **402**: 251 (1997)
44 S. A. Bass et al, Prog. Part. Nucl. Phys., **41**: 255 (1998)
45 M. Bleicher et al, J. Phys. G, **25**: 1859 (1999)
46 Z. W. Lin, C. M. Ko, B. An. Li, B. Zhang, and S. Pal, Phys. Rev. C, **72**: 064901 (2005)
47 W. Cassing and E. L. Bratkovskaya, Nucl. Phys. A, **831**: 215 (2009)
48 T. Hirano and Y. Nara, PTEP, **2012**: 01A203 (2012)
49 C. Gale, G. Bertsch, and S. Das Gupta, Phys. Rev. C, **35** 1666 (1987)
50 P. Danielewicz and S. Pratt, Phys. Rev. C, **53**: 249 (1996)
51 P. F. Kolb, J. Sollfrank, and U. W. Heinz, Phys. Lett. B, **459**: 667 (1999); P. F. Kolb, J. Sollfrank, and U. W. Heinz, Phys. Rev. C, **62**: 054909 (2000); H. Song and U. W. Heinz, Phys. Rev. C, **77**: 064901 (2008)
52 H. Petersen, J. Steinheimer, M. Bleicher, and H. Stoecker, J. Phys. G, **36**: 055104 (2009)
53 Y. B. Ivanov, Phys. Rev. C, **89**(2): 024903 (2014)
54 Y. Zhou, K. Xiao, Z. Feng, F. Liu, and R. Snellings, Phys. Rev. C, **93**(3): 034909 (2016)
55 Y. Nara, H. Niemi, A. Ohnishi, J. Steinheimer, X. Luo, and H. Stöcker, arXiv:1708.05617 [nucl-th]
56 A. Le Fevre, Y. Leifels, C. Hartnack, and J. Aichelin, arXiv:1611.07500 [nucl-th]
57 C. Pinkenburg et al (E895 Collaboration), Phys. Rev. Lett., **83**: 1295 (1999)
58 K. Filimonov et al (CERES/NA45 Collaboration), AIP Conf. Proc., **610**: 556 (2002)
59 Y. Nara, H. Niemi, J. Steinheimer, and H. Stoecker, Phys. Lett. B, **769**: 543 (2017)